

Stress induced monoclinic phase in epitaxial BaTiO₃ on MgO

I. B. Misirlioglu and S. P. Alpay^{a)}

Department of Materials Science and Engineering, University of Connecticut, Storrs, Connecticut 06269
and Institute of Materials Science, University of Connecticut, Storrs, Connecticut 06269

Feizhou He^{b)} and B. O. Wells

Department of Physics, University of Connecticut, Storrs, Connecticut 06269

(Received 7 June 2005; accepted 22 March 2006; published online 30 May 2006)

We present a detailed strain analysis of epitaxial ferroelectric films taking into account multiple sources of strain, including the lattice mismatch between the film and the substrate, thermal strains due to differences in the thermal expansion coefficients of the film and the substrate, and relaxation by the formation of interfacial dislocations. The lattice parameters of the film are calculated using a thermodynamic formalism coupled with the strain analysis. The theoretical model shows that epitaxial (001) BaTiO₃ films on (001) MgO are expected to display successive phase transformations with decreasing temperatures that are different than the bulk. This is verified experimentally for 50 nm thick (001) BaTiO₃ films grown on (001) MgO substrates at 720 °C using pulsed laser deposition. A synchrotron x-ray diffraction study displays two slope changes in the temperature dependence of the out-of-plane lattice constant. This indicates that two phase transformations exist in the film as a function of temperature with transition temperatures and lattice constants that are consistent with the theoretically predicted phases. Theoretical results show that the first transformation at around 270 °C corresponds to a paraelectric-ferroelectric transition. The ferroelectric phase has an orthogonal symmetry (*Amm2*) with in-plane polarization components. The transformation at around -20 °C is an *Amm2* ↔ *Pm* transition between two ferroelectric phases. The ferroelectric *Pm* phase is monoclinic compared to the rhombohedral *R3m* phase in bulk. © 2006 American Institute of Physics. [DOI: 10.1063/1.2198938]

I. INTRODUCTION

Ferroelectric perovskites have many unique physical properties that make them candidate materials for various applications such as nonvolatile memories, dynamic random access memories (DRAMs), tunable devices, and pyroelectric detectors. In the vicinity of a paraelectric-to-ferroelectric phase transformation, these materials possess many useful electrical properties as well as drastic variations in the structural characteristics. It has been shown both experimentally and theoretically that when ferroelectrics are deposited as thin films, all electrical and electromechanical properties vary significantly as functions of the internal stresses.¹⁻⁶ Internal stresses in thin films arise due to a variety of reasons, including the lattice mismatch between the film and the substrate in the case of lattice-matched films, differences between thermal expansion coefficients of the film and the substrate (thermal stresses), the self-strain of the phase transformation, and microstresses due to defects.

BaTiO₃ (BT) is the prototypical ferroelectric perovskite. In BT, the TiO₆ octahedra are linked in a regular cubic array forming the high-symmetry *Pm3m* prototype in the paraelectric state. In the ferroelectric state below the Curie tempera-

ture $T_C = 110$ °C, a spontaneous polarization arises due to the noncentrosymmetric displacement of Ti⁴⁺ and O²⁻ ions relative to Ba²⁺ ions (*P4mm*). Associated with the phase transformation at T_C , there is a self-strain proportional to the polarization. This self-strain essentially describes the cubic-tetragonal structural transformation in the crystal due to the emergence of a permanent polarization via atomic displacements. At room temperature (RT), the spontaneous polarization of bulk BT is 0.27 C/m² accompanied with an expansion of 0.67% along the easy axis of the polarization and a contraction of -0.22% in transverse directions.⁷ This corresponds to a tetragonality of 1.2%, where the tetragonality is defined as $\delta = (c - a)/a$, and c and a are the lattice parameters in the tetragonal ferroelectric state.

The structural variations as a result of the paraelectric-to-ferroelectric transition are quite different in epitaxial ferroelectric films. The experimental observations can be basically categorized into two broad groups. The first group contains results that do not display any structural characteristics of the ferroelectric-to-paraelectric phase transformation where the film remains tetragonal over a large temperature range. For example, when grown on (001) SrTiO₃ (ST) substrates with varying thicknesses, BT films are found to be tetragonal at the deposition temperature and remain tetragonal down to cryogenic temperatures.⁸⁻¹⁰ In these studies, a tetragonality greater than 6% is observed in 6.7 nm thick BT films on ST, more than five times of what it is in the bulk. The second group of results contains observations where the

^{a)}Author to whom correspondence should be addressed; electronic mail: p.alpay@ims.uconn.edu

^{b)}Present address: Canadian Light Source, University of Saskatchewan, Saskatoon SK S7N 0X4, Canada.

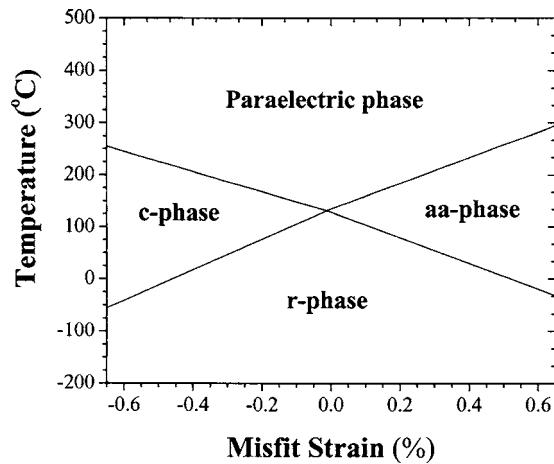


FIG. 1. Temperature-misfit strain phase diagram of the epitaxial (001) BT.

films are tetragonal at the deposition temperature but do display a variation in the structural characteristics at the critical temperature of the film^{5,11} which does not correspond to the transformation temperature in the bulk. These two cases appear to be incompatible. Among other goals, our present study should support one view or the other.

As all physical properties of ferroelectric thin films are directly a function of the internal strain state, it is important to understand the nature of structural changes due to phase transformations and relaxation mechanisms. In a recent study, we have carried out a comprehensive quantitative theoretical analysis based on a Landau-Devonshire (LD) thermodynamic model that shows that the phase transformation temperature, the lattice parameters, and the order of the phase transformation are strong functions of the internal stresses and are considerably different compared to unconstrained, unstressed single crystals of the same composition.¹² Depending on the internal stress state, it is possible that the structural aspects of the paraelectric-ferroelectric phase transformation may be completely obscured in the presence of epitaxial strains. This model also incorporates the stress relaxation at the deposition temperature by (interfacial) misfit dislocation generation as well as the effect of thermal stresses that may develop as the film is cooled down from the growth temperature T_G .

In this study, building upon our earlier work,¹² we include the possibility of the rotation of the polarization as a function of internal strain and temperature and report the results of a systematic theoretical and experimental investigation to explain the structural variations in ferroelectric films in the presence of biaxial epitaxial strains. Allowing the polarization of the film to adjust itself to changes in the stress conditions by rotating in all three dimensions may result in unusual phases not present in bulk ferroelectrics.¹³ Theoretical predictions combined with experimental observations based on a synchrotron x-ray diffraction analysis of the lattice parameters of a 50 nm thick (001) BT film on (001) MgO as a function of temperature suggest that it is possible to induce a monoclinic phase in epitaxial BT films at low temperatures.

II. THEORY

We will first begin with a comprehensive theoretical model to explain experimental observations of the lattice parameters of epitaxial (001) BT on (001) MgO substrate as a function of temperature. In this analysis, the measurement of the in-plane lattice parameter is used as an input to the thermodynamic model that yields the out-of-plane lattice parameter as a function of temperature as well as phase transformation temperatures.

A. Temperature-misfit strain phase diagram of (001) BT

The theoretical analysis starts with the construction of the temperature-misfit strain phase diagram of the epitaxial single-domain (001) BT film, details of which are described by Pertsev *et al.*¹³ (Fig. 1). Very briefly, a LD free energy functional is constructed where the biaxial stress state of an epitaxial ferroelectric film is coupled with the polarization vector P_i , the order parameter of the phase transformation. The formation of six possible phases due to the change in the symmetry as a result of the mechanical boundary conditions is predicted theoretically, compared to only four phases in bulk single crystals. These six phases are the *paraelectric* phase ($P_1=P_2=P_3=0$), the *c* phase ($P_1=P_2=0, P_3 \neq 0$), the *a* phase ($P_1 \neq 0, P_2=P_3=0$), the *ac* phase ($P_1 \neq 0, P_2=0, P_3 \neq 0$), the *aa* phase ($P_1=P_2 \neq 0, P_3=0$), and the *r* phase ($P_1=P_2 \neq 0, P_3 \neq 0$). The unusual *a*, *aa*, and the *ac* phases are in essence orientational variants of the ferroelectric tetragonal (*a* phase) and the orthorhombic (*aa* and *ac* phases) phases that are observed in bulk BT. The *c* and *a* phases are tetragonal (space group $P4mm$), the *aa* and *ac* phases are orthorhombic (space group $Amm2$), and the *r* phase in the film is monoclinic (space group Pm) compared to the rhombohedral phase with $P_1=P_2=P_3 \neq 0$ (space group $R3m$) in the bulk. Different from the phase diagram given by Pertsev *et al.*,¹³ we do not find a stability region of the *ac* phase. Our phase diagram is entirely consistent with recent first principles calculations of the strain phase diagram of BT where the *ac* phase was absent as well.^{14,15} We also note from Fig. 1 that in a particular epitaxial BT film, there can only be three distinct phases as a function of temperature, a reduction from four phases in the bulk BT.

B. Stress (strain) analysis

To describe structural variations, it is necessary to carefully analyze the stress state in the film. Epitaxy is characterized by mechanical boundary conditions corresponding to equal in-plane normal stresses ($\sigma_{11}=\sigma_{22}$), no shear stresses ($\sigma_{12}=\sigma_{13}=\sigma_{23}=0$), and no out-of-plane stress ($\sigma_{33}=0$). The vector and tensor quantities are defined in a Cartesian coordinate system with principal axes $x_1 \parallel (100)_{\text{film}}$, $x_2 \parallel (010)_{\text{film}}$, and $x_3 \parallel (001)_{\text{film}}$. The main parameter of the LD analysis is the in-plane misfit strain defined as $\epsilon_m = (a_S - a_0)/a_S$ where a_S is the substrate lattice parameter and a_0 is the equivalent

pseudocubic cell constant of the free standing unconstrained film.

However, this pseudocubic misfit is not the total strain. In the limit of linear elasticity, the total strain for a pseudomorphic film is

$$\varepsilon_{ij}^T = \varepsilon_{ij}^m + \varepsilon_{ij}^0. \quad (1)$$

Here,

$$\varepsilon_{ij}^0 = \begin{pmatrix} Q_{11}P_1^2 + Q_{12}(P_2^2 + P_3^2) & Q_{44}P_1P_2 & Q_{44}P_1P_3 \\ Q_{44}P_1P_2 & Q_{11}P_2^2 + Q_{12}(P_1^2 + P_3^2) & Q_{44}P_2P_3 \\ Q_{44}P_1P_3 & Q_{44}P_2P_3 & Q_{11}P_3^2 + Q_{12}(P_1^2 + P_2^2) \end{pmatrix}, \quad (3)$$

where Q_{ij} are the electrostrictive coefficients in the contracted notation. The self-strain describes the structural variation in an unconstrained crystal due to the atomic displacements in the crystal lattice that lead to a spontaneous polarization in the ferroelectric state. We note that depending on the type of a stable ferroelectric phase, there may be shear components of the self-strain, but they do not contribute to the total energy of the system because of the traction-free film surfaces, i.e., $\sigma_{12} = \sigma_{13} = \sigma_{23} = \sigma_{33} = 0$.

In epitaxial films and heterostructures, the strain due to the lattice mismatch between the film and the substrate can be partially or even completely relaxed during the film growth by the formation of orthogonal arrays of interfacial (or misfit) dislocations at the film-substrate interface. These dislocations are equilibrium defects, and their density and spacing depend on the film thickness, the nominal misfit, and the deposition temperature.¹⁶ Due to the relaxation by misfit dislocations, the internal stress state and thus the structural variations become a function of film thickness. The significance of the film thickness dependence of phase transformation characteristics have been very recently studied experimentally in detail for a variety of perovskite systems both in terms of structure and the order parameter of the transformation.¹⁷ Thermal stresses may also arise in the film as it is cooled down due to the differences between the thermal expansion coefficients (TECs) of the film and the substrate. These stresses usually cannot be relaxed by interfacial

$$\varepsilon_{ij}^m = \begin{pmatrix} \varepsilon_m & 0 & 0 \\ 0 & \varepsilon_m & 0 \\ 0 & 0 & [2S_{12}/(S_{11} + S_{12})]\varepsilon_m \end{pmatrix} \quad (2)$$

is a polarization-free misfit strain tensor where S_{ij} are the elastic compliances at a constant polarization in the contracted notation. The out-of-plane strain component follows from the mechanical boundary conditions.

ε_{ij}^0 is the self-strain tensor for a ferroelectric phase transformation and, in its most general form, is given by

defects due to kinetic reasons as the film cools down. The ultimate stress state in the film at ambient temperatures is thus due to an interplay between the dislocation induced relaxation at T_G and thermal stresses that develop afterwards as the film is cooled down. For example, because of this interplay it is possible to induce tensile in-plane stresses in a film on a “compressive” substrate, i.e., substrates with lattice parameters smaller than the film such that compressive stresses would have been induced in the plane of the film-substrate interface in pseudomorphic films, and vice versa.^{1,2}

The relaxation by misfit dislocations at the deposition temperature and the thermal stresses that develop during cooling down alter the strain state from the pseudomorphic case, as discussed above [Eq. (1)]. The total strain then becomes

$$\varepsilon_{ij}^T = \varepsilon_{ij}^m + \varepsilon_{ij}^0 + \varepsilon_{ij}^{\text{th}} + \varepsilon_{ij}^r + \varepsilon_{ij}^d. \quad (4)$$

In this relation,

$$\varepsilon_{ij}^{\text{th}} = \begin{pmatrix} \varepsilon_{\text{th}} & 0 & 0 \\ 0 & \varepsilon_{\text{th}} & 0 \\ 0 & 0 & [2S_{12}/(S_{11} + S_{12})]\varepsilon_{\text{th}} \end{pmatrix} \quad (5)$$

describes the thermal strain due to a temperature variation ΔT , where $\varepsilon_{\text{th}} = \Delta T(\alpha_{\text{film}} - \alpha_{\text{substrate}})$, with α_{film} and $\alpha_{\text{substrate}}$ being TECs of the film and the substrate, respectively.

ε_{ij}^r is the relaxation provided by the formation of misfit dislocations at T_G :

$$\varepsilon_{ij}^r = \begin{pmatrix} -\rho b \cos \lambda & 0 & 0 \\ 0 & -\rho b \cos \lambda & 0 \\ 0 & 0 & -[2S_{12}/(S_{11} + S_{12})]\rho b \cos \lambda \end{pmatrix}, \quad (6)$$

where b is the magnitude of the Burgers vector of the dislocation, λ is the angle between the Burgers vector and a vector in the plane of the film-substrate interface, and ρ is the linear dislocation density given by

$$\rho = \frac{\varepsilon_m(T_G)}{a_0(T_G)} \left(1 - \frac{h_p}{h}\right), \quad (7)$$

where h is the film thickness and h_p is the critical thickness for dislocation formation that can be determined theoretically from a classical Matthews-Blakeslee approach¹⁶ or experimentally. For cubic ferroelectric perovskites, the slip system is $\{010\}\{100\}$ based on transmission electron microscopy studies.^{18,19} Therefore, $\lambda=0^\circ$ and $b=a_0(T_G)$, and thus $\rho b \cos \lambda = \rho a_0(T_G)$.

The last term in Eq. (4), ε_{ij}^d , is the sum of the eigenstrains of the interfacial dislocations. These are microstrains or microdisturbances that, in accordance with the St. Venant's principle, extend only over a short range with a characteristic dimension of the order of $\sim 2b$. For films with $h \gg b$, the contribution of the self-strains to the overall strain state can safely be neglected. We note that the strain field around the dislocation also couples with the polarization, and their effect on all electrophysical properties becomes significant in ultrathin films.^{20,21}

C. Effective misfit, lattice parameters, and phase transformation temperatures

Equation (4) can be expressed in a more compact form as

$$\varepsilon_{ij}^T \cong \bar{\varepsilon}_{ij}^m + \varepsilon_{ij}^0, \quad (8)$$

where $\bar{\varepsilon}_{ij}^m = \varepsilon_{ij}^m + \varepsilon_{ij}^{\text{th}} + \varepsilon_{ij}^r$ is an effective misfit strain tensor that contains the relaxation by the formation of misfit dislocations at T_G and the thermal strains that develop subsequently. This temperature and film thickness dependent effective misfit $\bar{\varepsilon}_{ij}^m$ is given by

$$\bar{\varepsilon}_{ij}^m = \begin{pmatrix} \bar{\varepsilon}_m & 0 & 0 \\ 0 & \bar{\varepsilon}_m & 0 \\ 0 & 0 & [2S_{12}/(S_{11} + S_{12})]\bar{\varepsilon}_m \end{pmatrix}, \quad (9)$$

with an effective in-plane misfit

$$\bar{\varepsilon}_m(T, h) = \frac{\bar{a}_s(h, T) - a_0(T)}{\bar{a}_s(h, T)}, \quad (10)$$

where \bar{a}_s is an effective substrate lattice parameter²² expressed as

$$\bar{a}_s(h, T) = \frac{a_s(T)}{\rho(h, T_G)a_s(T) + 1}. \quad (11)$$

We note that for films with $h \gg h_p$, the in-plane misfit at T_G is completely relaxed since $\varepsilon_m(T_G) \approx \rho a_0(T_G)$ [see Eq. (7)]. The final strain state in such films, therefore, solely depends on the magnitude of thermal strains and the self-strain of the ferroelectric phase transformation, i.e.,

$$\varepsilon_{ij}^T \cong \varepsilon_{ij}^{\text{th}} + \varepsilon_{ij}^0. \quad (12)$$

The lattice parameters of the film can be theoretically determined from the relations given above. For epitaxial monodomain BT films the in-plane elastic clamping causes the in-plane parameter of the film to be equivalent to the effective substrate parameter irrespective of the self-strain of the ferroelectric transformation such that $a(h, T) \equiv \bar{a}_s(h, T)$. The out-of-plane lattice parameter of the film, $c(h, T)$, follows from

$$\varepsilon_{33}^T(h, T) = \frac{c(h, T) - a_0(T)}{c(h, T)} = \frac{2S_{12}}{S_{11} + S_{12}} \bar{\varepsilon}_m(h, T) + \varepsilon_{33}^0(T). \quad (13)$$

The temperatures at which phase transformations occur can be predicted from the phase diagram in Fig. 1. The phase border between the paraelectric and the aa phase essentially represents the temperature (T_{C1}) as a function of in-plane strain for in-plane components of the polarization to appear. It can be analytically expressed as¹³

$$T_{C1} = T_C + 2\varepsilon_0 C \left(\frac{Q_{11} + Q_{12}}{S_{11} + S_{12}} \right) \bar{\varepsilon}_m(T). \quad (14)$$

Similarly, the border between the paraelectric phase and the c phase as well as the border between the aa phase and the r phase represent the temperature (T_{C2}) as a function of in-plane strain where the out-of-plane component of polarization emerges¹³

$$T_{C2} = T_C + 4\varepsilon_0 C \left(\frac{Q_{12}}{S_{11} + S_{12}} \right) \bar{\varepsilon}_m(T). \quad (15)$$

III. EXPERIMENT

Pulsed laser deposition was used to grow (001) BT films on MgO (001) oriented single-crystal substrates. The energy density of the KrF excimer laser was about 1 J/cm². The films were grown at 720 °C in a 100 mTorr O₂ partial pressure. The thickness of the film used in this study was about 50 nm. X-ray diffraction (XRD) measurements were carried out at beamline X22A at the National Synchrotron Light Source, Brookhaven National Laboratory. X22A has a bent Si (111) monochromator, giving a small beam spot and a fixed incident photon energy of 10 keV. The angular resolution with a graphite (002) analyzer was less than 0.006° full width at half maximum (FWHM) for a (002) peak, as measured from the substrate. Below and above room temperature (RT=25 °C), the sample was cooled and heated in a high temperature capable displax with a base temperature near -263 °C, a maximum of 523 °C, and a temperature control of ± 0.5 °C.

The lattice parameters of BT films as a function of temperature obtained from the XRD measurements are given in Fig. 2, together with the parameters of bulk BT for comparison. Bulk BT transforms from the cubic paraelectric phase ($Pm3m$) to the ferroelectric tetragonal phase ($P4mm$) at around 110 °C upon cooling.²³ BT in the bulk undergoes two more phase transformations, from the tetragonal ferroelectric phase to an orthorhombic ferroelectric phase ($Amm2$) at 5 °C and then to the rhombohedral ferroelectric

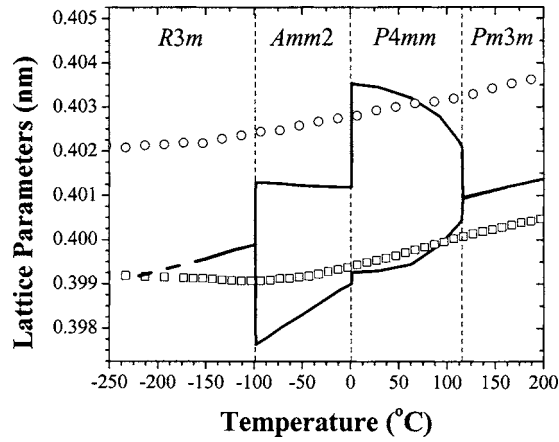


FIG. 2. Experimentally measured film lattice parameters of the 50 nm thick (001) BT on MgO (open circles: in plane; open squares: out of plane). Solid line corresponds to the lattice parameter of the bulk BT (see Ref. 7), with the vertical dashed lines denoting the phase transformation temperatures in the bulk.

phase ($R3m$) below -90 °C. In the unconstrained single-crystal BT, the tetragonality increases with the decreasing temperature, concurrent with the evolution of the spontaneous polarization below T_C . For the film, an entirely different behavior is observed with a negative tetragonality of -0.77% compared to 1.2% in the bulk at RT. Out-of-plane lattice parameter c shows gradual variations at two critical temperatures, approximately between 220 and 260 °C and -80 and -50 °C.

Our films were also analyzed to detect a polydomain formation (or twinning) using synchrotron x-ray diffraction. The samples did not display any peak splitting in the reciprocal space map of BT in the large temperature range of this study, which is an indication that our films are single-domain crystals. The polydomain formation has been observed in systems like PbTiO_3 and $\text{PbZr}_x\text{Ti}_{1-x}\text{O}_3$ in several structural characterization studies and has also been studied extensively theoretically.^{24–32} However, the generation of polydomain patterns in epitaxial BT films is rarely observed. In one of the few reports, Dai *et al.*³³ have shown that 90° domains only exist in the vicinity of interfacial dislocations in BT films grown on LaAlO_3 due to the highly localized large strain distribution around the dislocation core. These films certainly do not display a periodic polydomain pattern to relieve internal stresses, as predicted theoretically. This may be due to the interfacial elastic energy of domain walls and the electrostatic interaction between domains that are expected to increase the free energy of the system. Therefore, the theoretical analysis developed in the previous section for the stress state of the single-domain epitaxial ferroelectric films can be applied directly to explain the observed structural behavior of our 50 nm single-domain thick BT film on MgO.

IV. RESULTS AND DISCUSSION

To establish the link between the experimental results and the theory, we first note that the experimentally measured in-plane lattice parameter corresponds to the effective substrate parameter [Eq. (11)] due to clamping. Therefore,

TABLE I. The thermodynamic, elastic, and electrostrictive constants used in the theoretical modeling.

Constant	Minimum Value	Maximum Value
Q_{11} (m^4/C^2)	0.11 ^a	0.113 ^a
Q_{12} (m^4/C^2)	-0.029^a	-0.045^b
S_{11} ($\times 10^{-12}$ m^2/N)	7.35 ^c	11.2 ^d
S_{12} ($\times 10^{-12}$ m^2/N)	-1.39^c	-2.35^c

^aReference 34.

^bReference 13.

^cReference 37.

^dReference 38.

the in-plane strain of the film $\bar{\epsilon}_m$ [Eq. (10)] can be determined. It is worthwhile mentioning that Eqs. (11), (10), and (7) can be used to extract the dislocation density ρ of the film by plugging in the experimentally measured in-plane lattice parameter as the effective substrate parameter at T_G . The dislocation density of the as-grown film is essentially given by the deviation of the measured in-plane lattice parameter of the film at T_G from its bulk value. We estimate the linear dislocation spacing in our films to be ~ 9.5 nm. Were the films fully relaxed, the dislocation periodicity should be around 8 nm, indicating only a partial relief of the epitaxial strains in our film.

The polarization-free in-plane misfit strain $\bar{\epsilon}_m$ is the main parameter of the modified LD potential. Therefore, by extracting $\bar{\epsilon}_m$ from experimental data, all phase transformation characteristics, including the temperature dependence of the polarization in the BT layer, can be calculated. The thermodynamic parameters, the elastic moduli, and the electrostrictive coefficients used in the calculations are listed in Table I. The evolution of the polarization components is plotted along with the theoretical effective in-plane misfit strain as a function of temperature in Fig. 3. The film is, at first, under around 0.96% tension at T_G , and this changes when cooled down to cryogenic temperatures (to about 0.475% at $T = -250$ °C). This variation in the strain, together with the clamping effect, gives rise to strong variations of the polar-

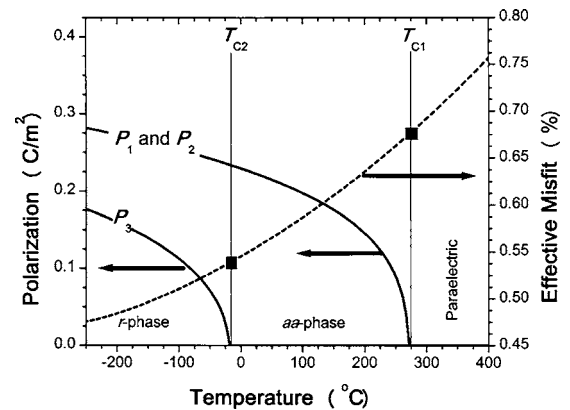


FIG. 3. The evolution of the theoretically determined polarization components as a function of temperature. The dashed line plots the polarization-free effective misfit. Intersection of T_{C1} and T_{C2} , with the misfit curves corresponding to the critical misfits at which the phase transformations occur.

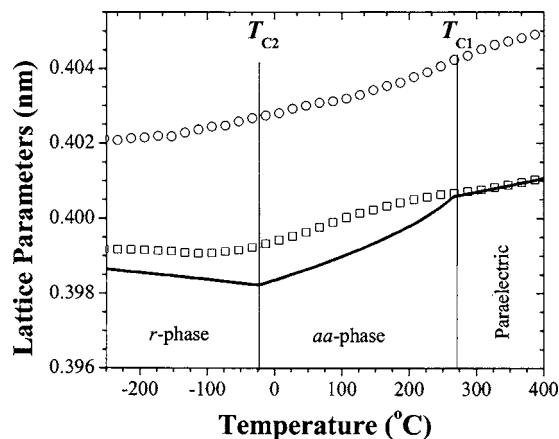


FIG. 4. Theoretically calculated lattice parameters of the 50 nm thick BT film on MgO as a function of temperature and the experimentally measured values. Open circles and squares are the experimentally measured values of a and c , respectively. The experimental in-plane lattice parameter a has been used as an input to theoretical calculations to predict the out-of-plane lattice parameter c .

ization components of the film with temperature and might result in phase transformations that are quite different than in the bulk BT.

As discussed above, the film at T_C is only partially relaxed. Using $\bar{\epsilon}_m$, we find that the film, although strained in plane and thus tetragonal, should not be ferroelectric starting from T_C down to around 270 °C. In accordance with the phase diagram, P_1 and P_2 are expected to emerge spontaneously at around 270 °C and are equal in magnitude to each other due to the biaxial in-plane misfit with equal strain components (Fig. 3). This phase transformation is distinctly different than the first ferroelectric phase transformation in bulk BT. In bulk BT, the paraelectric $Pm3m$ cubic phase transforms to the ferroelectric tetragonal ($P4mm$) phase at 110 °C.²³ In our film we predict that the first phase transformation upon cooling will be from a paraelectric tetragonal phase to an orthorhombic ($Amm2$) ferroelectric phase.

Theoretical calculations also predict that an out-of-plane component of polarization should develop at -20 °C with a 0.5% in-plane tensile misfit in addition to the in-plane components. The stable phase below -20 °C is the r phase (Pm). We emphasize that the r phase is monoclinic compared to the rhombohedral phase ($R3m$) in the bulk. The temperature evolution of the out-of-plane polarization P_3 is shown in Fig. 3.

The critical temperatures 270 and -20 °C for these two consequent phase transformations follow from Eqs. (14) and (15). These theoretical predictions are compatible with the experimental data. Examining the experimental results in Fig. 2, there are two inflection points where we observe slope changes in the evolution of the out-of-plane lattice parameter c . The theoretically determined transformation temperatures are close to the temperature ranges where the slope changes are observed, which are approximately between 220 and 260 °C and -80 and -50 °C, respectively (see Figs. 2 and 4). Indeed, if there were no phase transformations and thus no self-strain due to the appearance of polarization, c should follow changes in the thermal expansion of the in-plane lattice parameter a as a function of temperature as seen in ST films.¹⁷

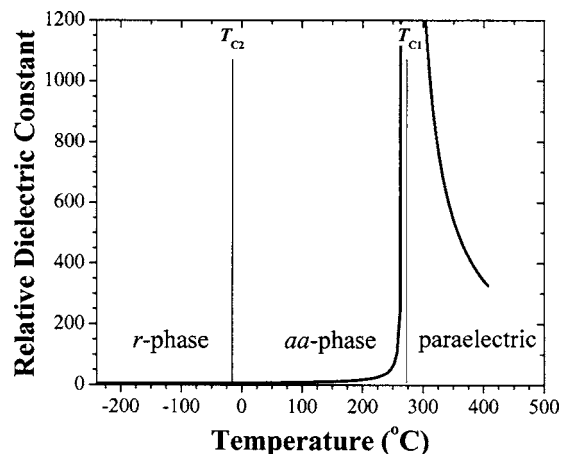


FIG. 5. Theoretical in-plane relative dielectric constant of the 50 nm thick (001) BT film on MgO.

The out-of-plane lattice parameter can now be calculated using Eq. (13) since both the polarization-free misfit ($\bar{\epsilon}_m$) and the out-of-plane self-strain due to the polarization in the ferroelectric state (ϵ_{33}^0) are known. In Fig. 4, we plot the theoretical lattice parameters of the epitaxial BT film as a function of temperature along with the experimental observations. The experimental data and theoretical results are in apparent agreement. We note that the literature contains a wide range of elastic constants and electrostrictive coefficients as listed in Table I. This is particularly true for the electrostrictive coefficient Q_{12} that plays a significant role in determining the self-strain due to the in-plane polarization components.^{13,34} To account for these variations we have carried out the calculations averaging the values of Q_{11} , Q_{12} , S_{11} , and S_{12} reported in literature (See Table I). The solid line represents the theoretical out-of-plane lattice parameter for the average of minimum and maximum values of the electrostrictive constants and elastic compliances.

We emphasize that the conclusions of this study are based on theoretical methods and measurements of the lattice parameters of BT as a function of temperature. Experimental observations and theoretical modeling are consistent with each other, but are by no means conclusive. Clearly, further experimental studies are needed to verify the presence of the aa and r phases in BT at certain in-plane stress states. A more detailed low-temperature XRD analysis is underway to identify the crystal structure of the BT film in this study below T_{C2} . Structural studies should be supported with electrical measurements as a function of temperature to prove the existence of ferroelectricity. These can be achieved by determining the dielectric response or the polarization hysteresis loops as a function of temperature. For example, in Fig. 5 we plot the theoretical in-plane relative dielectric constant (κ_{11}) of the BT film in this study as a function of temperature.^{2,13}

The peak in κ_{11} around T_{C1} corresponds to the emergence of the in-plane components P_1 and P_2 of the ferroelectric orthorhombic aa phase. Below T_{C1} , the film should display a ferroelectric hysteresis in its polarization versus applied electrical field behavior in the plane of the film-substrate interface. The possibility of the formation of a monoclinic phase in epitaxial (110) $Ba_{0.6}Sr_{0.4}TiO_3$ (BST) films on (100)

NdGaO₃ has also been discussed very recently by Simon *et al.*³⁵ In this study, x-ray pole figures combined with in-plane dielectric measurements along several crystallographic directions seem to suggest that the room temperature crystal structure of BST is monoclinic due to the anisotropic epitaxial strain.

To benefit from the electrical properties in a desired manner in technological applications of ferroelectric films, accurate predictions and measurements of the phase transformations and the transformation temperatures become very important factors. For example, the in-plane polarization components play a crucial role in varactor capacitor applications with interdigitated electrodes that supply an electrical field along in-plane directions in the film-substrate interface. Therefore, the stress state in ferroelectric films should be carefully evaluated, and this analysis has to incorporate the contributions from various sources such as interfacial dislocations, the self-strain of the phase transformation, and the difference between the TECs. In cases where there is no apparent structural variation (such as in BT films on ST substrates^{8,36}), this should not be ascribed to the absence of the ferroelectric phase transformation, and electrical measurements should be conducted to supplement XRD observations.

V. CONCLUSIONS

Structural characteristics of (001) BT films on (001) MgO substrates were investigated using a detailed strain analysis, thermodynamic modeling, and XRD synchrotron studies. Out-of-plane polarization components were calculated, and their evolution with temperature was determined. The theoretical out-of-plane lattice parameter of the BT film follows experimental observations closely throughout the wide temperature range of measurement. Theoretical and experimental results point out the presence of two phase transformations in these films and suggest the formation of a monoclinic ferroelectric phase at low temperatures approximately in the -80 and -50 °C range. The calculation does a good job predicting the observed temperature variation of the out-of-plane lattice parameter.

ACKNOWLEDGMENTS

This material is based upon work supported by the National Science Foundation under Grant Nos. DMR-0132918 (I.B.M. and S.P.A.) and DMR-0239667 (B.O.W. and F.H.). One of the authors (B.O.W.) also thanks the Cottrell Scholar Program of the Research Corporation for partial support of this work.

- ¹A. L. Roytburd, S. P. Alpay, V. Nagarajan, C. S. Ganpule, S. Aggarwal, E. D. Williams, and R. Ramesh, *Phys. Rev. Lett.* **85**, 190 (2000).
- ²Z. G. Ban and S. P. Alpay, *J. Appl. Phys.* **91**, 9288 (2002).
- ³T. M. Shaw, Z. Suo, M. Huang, E. Liniger, R. B. Laibowitz, and J. D. Baniecki, *Appl. Phys. Lett.* **75**, 2129 (1999).
- ⁴C. L. Canedy, H. Li, S. P. Alpay, L. Salamanca-Riba, A. L. Roytburd, and R. Ramesh, *Appl. Phys. Lett.* **77**, 1695 (2000).
- ⁵K. J. Choi *et al.*, *Science* **306**, 1005 (2004).
- ⁶V. Nagarajan, C. S. Ganpule, B. Nagaraj, S. Aggarwal, S. P. Alpay, A. L. Roytburd, E. D. Williams, and R. Ramesh, *Appl. Phys. Lett.* **75**, 4183 (1999).
- ⁷E. Fatuzzo and W. J. Merz, *Ferroelectricity* (North-Holland, Amsterdam, 1967).
- ⁸H. Terauchi, Y. Watanabe, H. Kasatani, K. Kamigaki, Y. Yano, T. Terashima, and Y. Bando, *J. Phys. Soc. Jpn.* **61**, 2194 (1992).
- ⁹Y. Yoneda, H. Kasatani, H. Terauchi, Y. Yoshihiko, T. Terashima, and Y. Bando, *J. Cryst. Growth* **150**, 1090 (1995).
- ¹⁰Y. Yoneda, T. Okabe, K. Sakaue, and H. Terauchi, *Surf. Sci.* **410**, 62 (1998).
- ¹¹F. M. Bai, H. M. Zheng, H. Cao, L. E. Cross, R. Ramesh, J. F. Li, and D. Viehland, *Appl. Phys. Lett.* **85**, 4109 (2004).
- ¹²S. P. Alpay, I. B. Misirlioglu, A. Sharma, and Z. G. Ban, *J. Appl. Phys.* **95**, 8118 (2004).
- ¹³N. A. Pertsev, A. G. Zembilgotov, and A. K. Tagantsev, *Phys. Rev. Lett.* **80**, 1988 (1998).
- ¹⁴B. K. Lai, I. A. Kornev, L. Bellaiche, and G. J. Salamo, *Appl. Phys. Lett.* **86**, 132904 (2005).
- ¹⁵O. Dieguez, S. Tinte, A. Antons, C. Bungaro, J. B. Neaton, K. M. Rabe, and D. Vanderbilt, *Phys. Rev. B* **69**, 212101 (2004).
- ¹⁶J. W. Matthews and A. E. Blakeslee, *J. Cryst. Growth* **27**, 118 (1974).
- ¹⁷F. He *et al.*, *Phys. Rev. B* **70**, 235405 (2004).
- ¹⁸T. Suzuki, Y. Nishi, and M. Fujimoto, *Philos. Mag. A* **79**, 2461 (1999).
- ¹⁹I. B. Misirlioglu, A. L. Vasiliev, M. Aindow, S. P. Alpay, and R. Ramesh, *Appl. Phys. Lett.* **84**, 1742 (2004).
- ²⁰S. P. Alpay, I. B. Misirlioglu, V. Nagarajan, and R. Ramesh, *Appl. Phys. Lett.* **85**, 2044 (2004).
- ²¹V. Nagarajan, C. L. Jia, H. Kohlstedt, R. Waser, I. B. Misirlioglu, S. P. Alpay, and R. Ramesh, *Appl. Phys. Lett.* **86**, 192910 (2005).
- ²²S. P. Alpay, V. Nagarajan, A. Bendersky, M. D. Vaudin, S. Aggarwal, R. Ramesh, and A. L. Roytburd, *J. Appl. Phys.* **85**, 3271 (1999).
- ²³F. Jona and G. Shirane, *Ferroelectric Crystals* (Dover, New York, 1993).
- ²⁴A. L. Roytburd, *Phys. Status Solidi A* **37**, 329 (1976).
- ²⁵B. S. Kwak, A. Erbil, J. D. Budai, M. F. Chisholm, L. A. Boatner, and B. J. Wilkens, *Phys. Rev. B* **49**, 14865 (1994).
- ²⁶S. Kim and S. Baik, *Thin Solid Films* **266**, 205 (1995).
- ²⁷N. A. Pertsev and A. G. Zembilgotov, *J. Appl. Phys.* **78**, 6170 (1995).
- ²⁸V. G. Koukhar, N. A. Pertsev, and R. Waser, *Phys. Rev. B* **64**, 214103 (2001).
- ²⁹S. P. Alpay and A. L. Roytburd, *J. Appl. Phys.* **83**, 4714 (1998).
- ³⁰N. A. Pertsev and V. G. Koukhar, *Phys. Rev. Lett.* **84**, 3722 (2000).
- ³¹Y. M. Kang, K. S. Lee, and S. Baik, *Ferroelectrics* **196**, 325 (1997).
- ³²Y. M. Kang and S. Baik, *J. Appl. Phys.* **82**, 2532 (1997).
- ³³Z. R. Dai, Z. L. Wang, X. F. Duan, and J. Zhang, *Appl. Phys. Lett.* **68**, 3093 (1996).
- ³⁴T. Mitsui, E. Nakamura, and K. Gesi, *Numerical Data and Functional Relationships in Science and Technology*, edited by K.-H. Hellwege and A. M. Hellwege, Landolt-Börnstein, New Series, Group 3, Vol. 16 (Springer, Berlin, 1981).
- ³⁵W. K. Simon, E. K. Akdogan, A. Safari, and J. A. Belotti, *Appl. Phys. Lett.* **87**, 082906 (2005).
- ³⁶S. S. Kim and J. H. Je, *J. Mater. Res.* **14**, 3734 (1999).
- ³⁷Z. Li, S.-K. Chan, M. H. Grimsditch, and E. S. Zouboulis, *J. Appl. Phys.* **70**, 7327 (1991).
- ³⁸D. Berlincourt and H. Jaffe, *Phys. Rev.* **111**, 143 (1958).